Aerosol Science and Technology

ISSN: 0278-6826 (Print) 1521-7388 (Online) Journal homepage: http://www.tandfonline.com/loi/uast20

Vortices in Anisoaxial Sampling Inlets

Chih-Chieh Chen & Paul A. Baron

To cite this article: Chih-Chieh Chen & Paul A. Baron (1995) Vortices in Anisoaxial Sampling Inlets, Aerosol Science and Technology, 23:2, 224-230, DOI: 10.1080/02786829508965305

To link to this article: https://doi.org/10.1080/02786829508965305

Vortices in Anisoaxial Sampling Inlets*

Chih-Chieh Chen† and Paul A. Baron
U.S. Department of Health and Human Services
Public Health Service,
Centers For Disease Control and Prevention,
National Institute for Occupational Safety and Health,
Division of Physical Sciences and Engineering,
Cincinnati, OH 45226, USA

Thin-walled inlets are used in a variety of instruments and sampling devices, quite often under anisoaxial conditions. An earlier study demonstrated a new visualization technique for observing vortices formed in a tubular inlet and indicated the effect of varying sampling rate and angle. The effect of the flow patterns on gravitational settling, inertial separation, and electrostatic interaction was observed. The present study extends this work by examining these effects over a wider range of sampling conditions and for some different inlet configurations. The vortices formed as a result of anisoaxial sampling change their location and increase in intensity and size with increasing external air velocity. The vortices appear even for relatively short inlets. A flared inlet appears to eliminate the vortices for sampling angles of less than 90°.

INTRODUCTION

Vortices can form during anisoaxial sampling with thin-walled samplers. In an earlier study (Baron et al. 1994), we investigated the flow patterns in a fiber sampler under a limited set of air flow conditions. The patterns showed that vortices are formed with increasing size at higher sampling angles and with increasing intensity (higher rotational velocity) at higher sampling velocities. The location and shape of the vortices were indicated using a unique visualization technique that showed the modification of the streamline trajectories by the entry into the inlet. Various mechanisms that cause particles to deviate from the flow streamlines, such as gravitational settling, inertial motion, or electrostatic interaction, were shown to be modified by the vortices to give nonuniform particle distributions within the inlet.

Redistribution of aerosol particles within the flow field under such anisoaxial conditions can introduce unexpected errors. Some instruments and measurement techniques are only accurate with a uniform particle distribution within the inlet, e.g., when only a small portion of the aerosol in the inlet is analyzed. For example, quantitative fiber analysis of filter samples by microscopy assumes that the collected fibers are distributed uniformly over the filter surface (Carter et al. 1984).

The present study further investigates the flow effects over a wider range of inlet conditions and inlet configurations.

EXPERIMENTAL METHODS

Two techniques were used for detecting flow patterns within an inlet: observation

*Mention of product or company name does not constitute endorsement by the Centers for Disease Control and Prevention.

†Current address: National Taiwan University, Taipei, Taiwan

0278-6826/95/$9.50
SSDI 0278-6826(94)00092-G

Aerosol Science and Technology 23:224-230 (1995)

Published by Elsevier Science Inc.

of smoke streams entering the inlet and observation of patterns deposited on a filter in the sampling inlet. The smoke stream observation is a commonly used technique for assessing flow patterns (White 1986). A two-dimensional light sheet was created with a HeNe laser and a cylindrical lens (straight-line generator lens, Edmund Scientific, Barrington, NJ). A thin smoke stream was injected into the center of the 20-cm-diameter chamber, which was 1 m long with a porous foam and honeycomb flow straightener. The flow in and around the inlet was illuminated with the light sheet at several angles. A video camera and 35-mm camera were used to visually document the effect of sampler configurations on the introduced smoke stream.

The second technique involved generating charged 3-μm and 10-μm aerodynamic diameter (d_{ae}) methylene blue particles with a vibrating orifice aerosol generator (VOAG, model 3400, TSI, Inc., St. Paul, MN). The generator was modified according to Reischl et al. (1977), creating monodisperse particles with a uniform unipolar charge. A hexagonal grid pattern was superimposed onto this aerosol flow using the technique in our earlier study (Baron et al. 1994). The chamber used in that study was modified with an added sheath flow section after the generator, but before the flow straightener to increase the wind velocity through the sampling region. This arrangement kept the aerosol concentration reasonably high near the axis of the chamber where the sampling was performed.

The chamber aerosol flow in these experiments was moving vertically downward. The sampling angle (θ) was defined as the angle between the air motion in the chamber and the air motion in the inlet axis (Fig. 1a). Thus, $\theta = 0°$ for the sampler inlet under isoaxial conditions. Note that the angle relative to gravity is also equal to θ.

In most of the experiments, the inlet used was the fiber sampling cassette (Millipore Corp., Bedford, MA), which is 50 mm long with a nominal 25 mm diameter. The sampler was slightly conductive due to its graphite-loaded plastic composition. The inlet wall thickness was 2 mm at the inlet face. The ratio of outer diameter (D) to inner inlet diameter (d) ($D/d = 1.15$) was close to that used as the definition of a thin-walled inlet ($D/d \leq 1.1$) (Belyaev and Levin 1974). Thus, the inlet approximated a thin-walled inlet. At least two samples were taken at each condition for two particle sizes ($d_{ae} = 3$ μm and 10 μm), a range of angles ($\theta = 0°$–$150°$), flow rates (0.5–10 L/min; corresponding inlet velocity $U_i = 1.6$–32 cm/s), and external velocities ($U_w = 5$–100 cm/s). Several other sampler configurations were also tested: two shorter inlets (27 mm and 18 mm long), and a flared inlet (Bellmouth cowl, Envirometrics, Charleston, SC). Sampling times ranged from about 2 min for 10-μm particles, high sampler flow, and low chamber velocity to several hours for 3-μm particles, low sampler flow, and high chamber velocities.

OBSERVATIONS

Observation of the smoke stream patterns was used to provide an indication of the flow patterns both outside and inside the sampler inlet. The laser light sheet provided more detailed illumination of the flow patterns than the white light source used in the previous study. The streamlines were largely similar to those observed in that study. A streamline entering the downstream side of the inlet made a smooth turn and entered the inlet relatively undisturbed (Fig. 1b). The streamlines entering the upstream side of the tubular inlet for $\theta > 90°$ formed vortices. The combination of the laser light sheet and video tape playback showed that particles in the vortex formed at the inlet

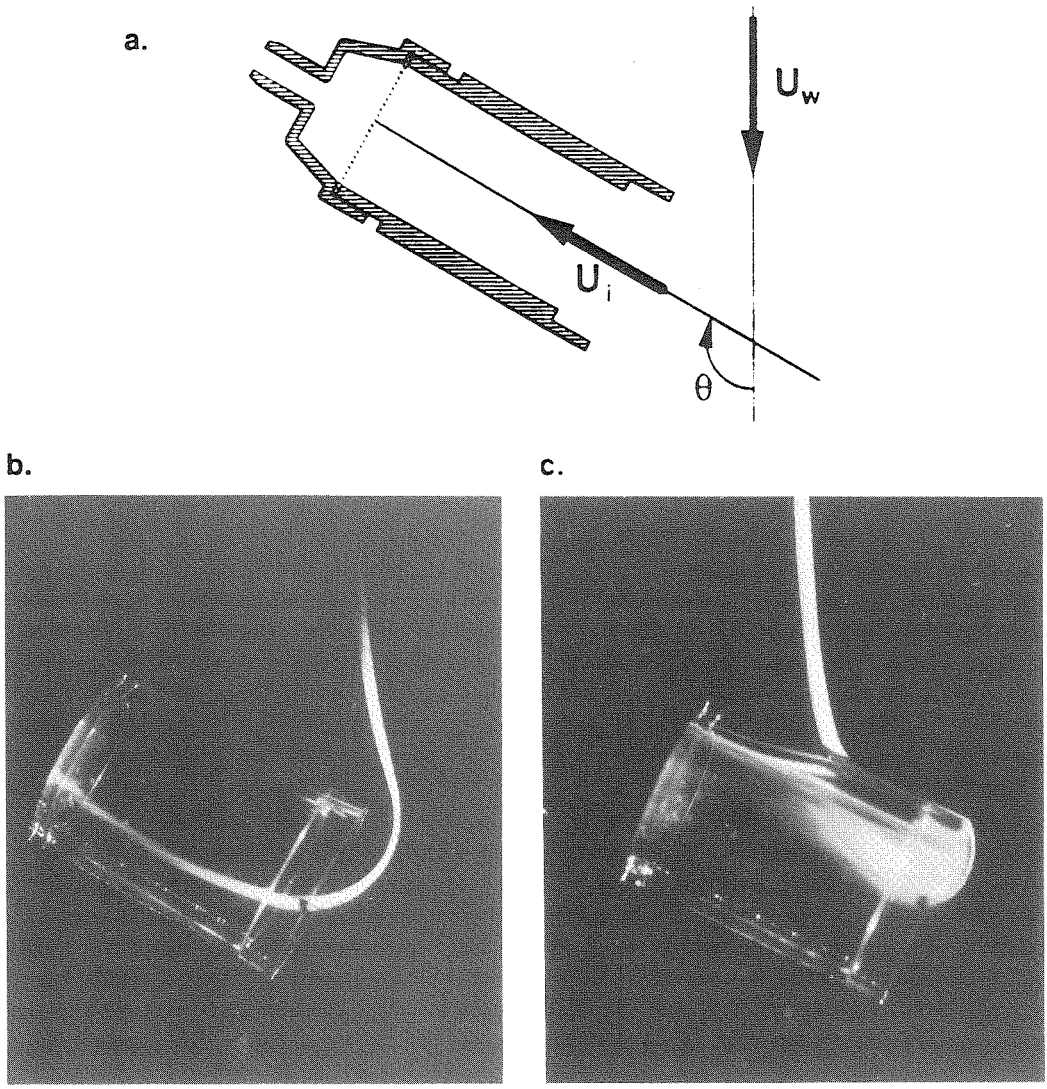

FIGURE 1. Pictures of smoke stream observations with the laser light sheet at a sampling angle of 120°: (a) coordinate frame for inlet velocity (U_i), wind velocity (U_w), and sampling angle (θ); (b) external velocity 17 cm/s, inlet velocity 17 cm/s; (c) same conditions as (b) but streamline initially aimed at the center of the cassette.

appeared to recirculate in an eddy, thus keeping particles near the inlet for an extended time. At high sampling flow rates, this recirculation pattern was elongated (Fig. 1c), while at low flow rates, it became more circular and was situated near the face of the inlet. At higher wind speeds, the overshoot of the streamline past the leading edge of the inlet also increased. Vortex shedding downwind of

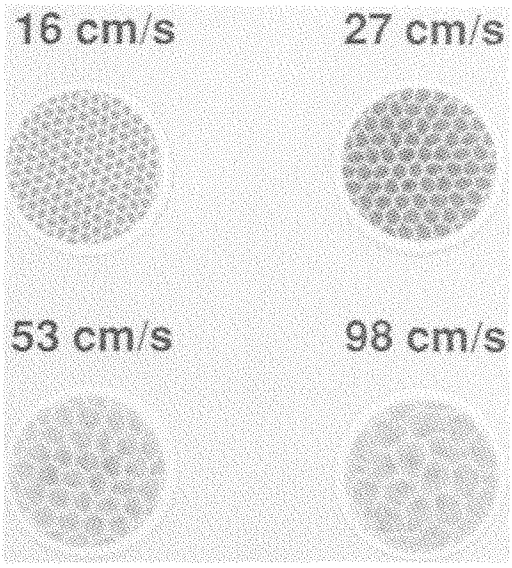

FIGURE 2. Filter deposits from isoaxial sampling with inlet velocity of 32 cm/s. The hexagonal pattern is due to electrostatic repulsion of particles from the honeycomb flow straightener upstream of the sampler. The grid pattern size is a function of the relative velocity between the air velocity at the flow straightener and at the filter surface.

the sampler occurred at all experimental conditions and increased in intensity with increasing wind velocity.

Cross-sectional views of the streamlines were observed using the technique developed in our earlier study whereby the streamlines were represented by a hexagonal pattern in the aerosol stream. The hexagonal patterns were formed due to charged particle interaction with charged honeycomb flow straighteners upstream of the sampler. Although a large number of filter deposition patterns were observed, only a few are presented here because of the similarity to figures presented previously. Shown in Fig. 2 are examples of four filter deposits of methylene blue collected at isoaxial conditions with U_w = 16–90 cm/s for $U_i = 32$ cm/s. Filter samples collected with three different inlet configurations at $\theta = 90°$ and 120°, and $U_i = U_w = 32$ cm/s are shown in Fig. 3. Two filter patterns of samples taken at low inlet velocity ($U_i = 14$ cm/s, $U_w = 34$ cm/s) with $\theta = 60°$ and 120° are shown in Fig. 4.

DISCUSSION

The observed smoke stream trajectories passing through the vortices were complex. The streamline observations depended to some extent on the thickness of the smoke stream and were difficult to follow in a quantitative manner. In addition, the laser sheet gave only a two-dimensional view of the smoke pattern so that it was difficult to precisely determine the path of the three-dimensional motion of the air streamlines (Figs. 1a and 1b). The general trends observable were largely in agreement with results reported in the previous study. However, recirculation appeared to occur along the inlet axis, resulting in longer residence times of particles in the inlet, which could further enhance sampling bias mechanisms, especially electrostatic deposition or repulsion.

The hexagonal pattern technique observed on the filter deposit was extended to wind velocities of 100 cm/s (Fig. 2). These patterns were obtained with the 3-μm particles, which had small enough inertia to follow the streamlines in these measurements. The patterns were still quite clear at 100 cm/s, though the sampling time required to obtain an observable pattern at these velocities increased to as much as 2 h for 3-μm particles with a low inlet sampling rate. Some distortion of the pattern was observable, apparently due to small but stable velocity variations in the chamber flow. Attempts at sampling at higher wind velocities were not successful in producing clearly defined streamline patterns.

The vortex development along the length of the inlet was observed by using

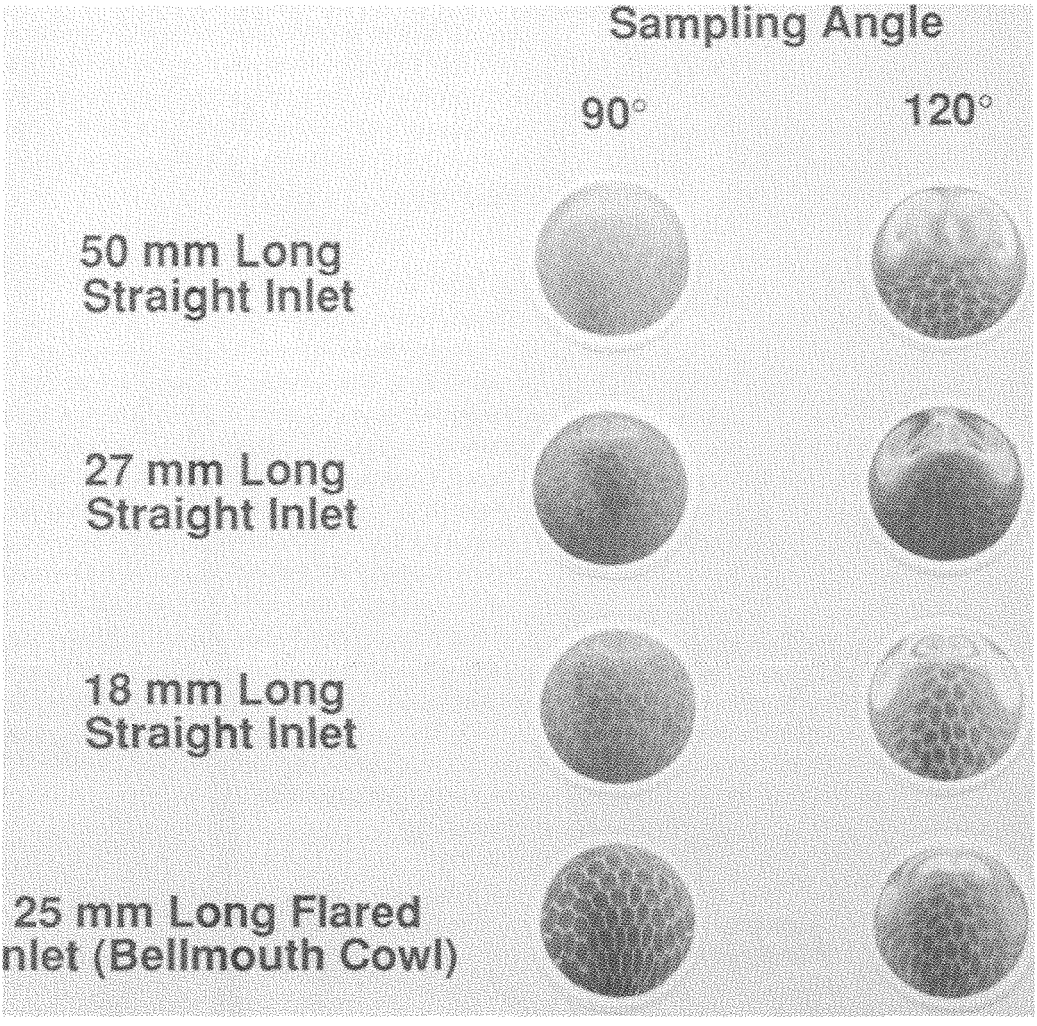

FIGURE 3. Filter deposits at 90° and 120° for four inlet configurations with external and inlet velocities of 32 cm/s: The original 50-mm-long inlet; the inlet shortened to 27 mm; the inlet shortened to 18 mm; and a Bellmouth sampler, which is 25 mm long and flared.

inlets of various lengths. Figure 3 shows patterns developed at three inlet lengths at 90° and 120°. The sharpness of the vortex pattern decreased with increasing inlet length, especially at 120° and higher; this was probably caused by small flow pattern instabilities that were magnified over the length of inlet. Since the patterns were fully developed even for the shortest inlet, the vortices appeared to be formed at the front surface of the inlet by the interaction of the inlet shape and the internal and external airflows. At high U_w, the patterns also lost clarity and were observed as simply a region of decreased particle deposition. For example, at $\theta = 120°$, $U_w = 85$ cm/s, $U_i = 34$ cm/s, no vortices were evident in deposition patterns,

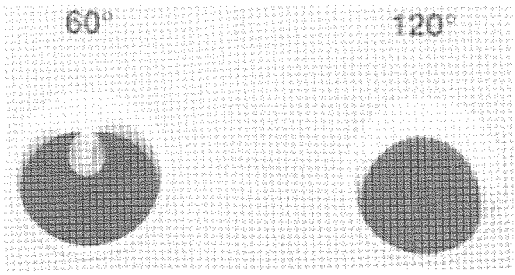

FIGURE 4. The interaction of sedimentation and the vortices. External velocity was 34 cm/s, inlet velocity was 14 cm/s, and particle size was 10 μm. Sample angles (θ) are indicated.

but a lighter region indicating the extent of the vortices covered all but a crescent-shaped region (3 mm thick at the center) at the downstream side of the filter.

A commercially available flared inlet (Bellmouth cowl) was also evaluated. The deposition patterns for the flared inlet showed no vortices at angles up to 90° (Fig. 3), indicating that the outward flare allowed air to enter more smoothly. However, at 120° a complex flow pattern similar to that of the straight inlet was formed. Although a slight distortion of the hexagonal pattern was observed at 90°, the absence of a vortex indicates that this type of inlet may have improved sampling characteristics over a straight inlet at $\theta \leq 90°$.

The implications of vortex formation when combined with various inertial, gravitational, and electrostatic forces were discussed in the previous study. For sample measurement techniques that require uniform sample distribution within the inlet, improved accuracy can be achieved by eliminating these vortices. In workplace or environmental sampling, an inlet, such as the Bellmouth cowl, might provide better results, especially if the external wind direction were constrained to be less the 90° by a shield or appropriate sampling strategy. Measurements of air velocities in several workplaces by Berry and Froude (Berry et al. 1989) were consistent with air currents in these locations being directed horizontally most of the time. Thus, an area sampler with a flared inlet pointing vertically up or down might reduce vortex formation by preventing sampling at angles significantly larger than 90°. Personal samplers worn by a worker might also be improved by placing such a sampler so that the inlet faced 90° to the body surface. This orientation would constrain airflow into the inlet to less than about 90°.

A study investigating asbestos fiber uniformity on filter samples found that a sampler with the Bellmouth cowl provided more uniform filter deposits for isoaxial, subisokinetic sampling ($U_w/U_i = 0.38$) when compared with the standard tubular inlet (Feigley et al. 1992). While the flare inlet appears to give more uniform filter deposits, the inlet aspiration efficiency of this sampler has not been investigated as thoroughly as the tubular inlet. Further work needs to be done in this area.

Our earlier measurements indicated that at a low external velocity (14 cm/s) the vortices increase in size with decreasing inlet velocities (U_w/U_i increasing). In this study, a similar trend was noted, i.e., increasing vortex size with increasing U_w/U_i. In addition, the vortex patterns on the filter appeared to be more poorly defined with higher external velocities.

The flow patterns displayed in Fig. 3 was primarily due to the hexagonal pattern impressed on the aerosol upstream of the sampler. However, since these patterns were obtained at a sampling angle of 120°, additional losses of particles may have occurred in the region where the particles passed near the outer surface of the sampler (see Fig. 1c). When charged particles pass near a conductive surface, image charge attraction to the surface occurs. A loss to the outer wall, estimated to be on the order of 1–3%, enhanced the width of the particle-free regions in the vortex patterns.

Sedimentation has been observed using a filter deposition technique similar to the one in the present study in horizontal tubes (Thomas et al. 1967). Theoretical penetration efficiencies have been calculated for tubes at various angles to the horizontal (Heyder et al. 1977). For inlets that are not facing straight upwards, sedimentation tends to form a crescent-shaped particle-free region of increasing width along the length of the inlet (Fig. 4b). This region can mix with the vortices under anisoaxial sampling to create a more complex particle distribution pattern (Fig. 4a). The $\theta = 120°$ sample may be showing some effect of the vortices as indicated by the blurring of the pattern near the ends of the crescent, but the final pattern is dominated by particle settling. On the $\theta = 60°$ sample a nearly circular particle-free area shows up near the center of the filter due to the vortices. Such a particle pattern would cause large biases if the aerosol were samples in the center of the inlet. A less intense pattern is also seen superimposed on the darker pattern in Fig. 4a. This pattern may be due to a smaller vortex that is formed in the center of the particle-free circular region of the more intense pattern. However, based on its intensity and its apparent superposition on the more intense pattern, it may also be due to doublet particles (double-volume particles produced by coagulation) formed in the VOAG that interact differently with the vortex pattern.

The observation of the inlet flow patterns and particle deposition patterns has some implications for inlets currently in use. Some measurements assume that the particle distribution in the inlet is uniform. For instance, fiber measurements are performed with the sampling inlet used in this study. The analysis is performed on small, randomly selected portions of the filter and is clearly subject to increased variability and bias due to the vortices and various mechanisms discussed above. Other samplers may take a small portion of the inlet flow for analysis. For instance, the Aerodynamic Particle Sizer (TSI, Inc., St. Paul) has a primary inlet sampling at 5 L/min and a centered secondary inlet downstream that samples the aerosol at 1 L/min. Thus, one must be careful in sampling and ducting the aerosol to the instrument to avoid serious biases, especially for larger or charged particles.

The authors gratefully acknowledge the assistance of Mary Kathleen Eley in performing some of the measurements.

REFERENCES

Baron, P. A., Chen, C. C., Hemenway, D. R., and O'Shaughnessy, P. (1994). *Am. Ind. Hyg. Assoc. J.* 55(8):722–732.

Belyaev, S. P., and Levin, L. M. (1974). *J. Aerosol Sci.* 5:325–338.

Berry, R. D., and Froude, S. (1989). Report IR/L/DS/89/3, UK Health and Safety Executive.

Carter, J., Taylor, D., and Baron, P. A. (1984). Fibers, Method 7400, Issue 2; in *NIOSH Manual of Analytical Methods*. DHHS (NIOSH). 3rd ed. Cincinnati, OH.

Feigley, C. E., Maguire, K. E., Hussey, J. R. (1992). *Appl. Occup. Environ. Hyg.* 7(11):749–757.

Heyder, J., and Gebhart, J. (1977). *J. Aerosol Sci.* 8:289–295.

Reischl, G., John, W., and Devor, W. (1977) *J. Aerosol Sci.* 8:55–65.

Thomas, J. W., Knuth, R. H. (1967). *Am Ind. Hyg. Assoc. J.* 28(May–June):229–237.

White, F. M. (1986). *Fluid Mechanics*. New York, McGraw-Hill.

Received April 24, 1994; revised November 9, 1994.